Theoretical and experimental study of polarization switching in long-wavelength VCSELs subject to parallel optical injection

A. Quirce*[a], P. Pérez[b], A. Popp[b], A.Valle[b], L. Pesquera[b], Y. Hong[c], H. Thienpont[a], K. Panajotov[a,d]

[a]Vrije Universiteit Brussel, Faculty of Engineering Sciences, Brussels Photonics Team B-PHOT, Pleinlaan 2, 1050 Brussels, Belgium
[b]Instituto de Física de Cantabria, CSIC-Universidad de Cantabria, Avda. Los Castros s/n, 39005, Santander, Spain
[c]School of Electronic Engineering, Bangor University, Gwynedd LL57 1UT, Wales, UK
[d]Institute of Solid State Physics, 72 Tzarigradsko, Chausse Blvd., 1784, Sofia, Bulgaria

ABSTRACT

We report a theoretical and experimental analysis of the polarization switching found in a single-transverse mode VCSEL when subject to parallel optical injection. We have found a novel situation in which injection locking of the parallel polarization and excitation of the free-running orthogonal polarization of the VCSEL are simultaneously obtained. Analytical expressions for the power of both linear polarizations in the previous steady state are determined. We show that considering two linear polarization modes in a model of a VCSEL subject to parallel optical injection leads to simpler expressions than those found for a VCSEL with only a single linear polarization. We show that the power emitted in both linear polarizations depend linearly on the injected power. The stability region of this solution is measured in the plane injected power versus frequency detuning.

Keywords: Vertical-Cavity Surface-Emitting Laser (VCSEL), Polarization, Non-linear Dynamics, Injection-locking.

1. INTRODUCTION

Semiconductor lasers can be easily destabilized by the introduction of external perturbations such as optical injection, external optical feedback or modulation of laser parameters [1]. The availability and ease of operation of semiconductor lasers make them a convenient test-bed for exploring basic aspects of nonlinear dynamics [2]. Optical injection in semiconductor lasers has also been used to improve the performance of these devices without modifying their design [3-5]. Locking of the frequency of the injected laser to the one of the injecting laser has been used for the reduction of the laser linewidth or for an enhancement of its modulation bandwidth [3-5]. Nonlinear dynamics of optically injected semiconductor lasers has also been used for photonic microwave generation [6-8].

A lot of attention has been paid to the effects of optical injection on a special type of semiconductor laser: the vertical-cavity surface-emitting laser (VCSEL) [9-22]. VCSELs have demonstrated many impressive characteristics including low threshold currents, high coupling efficiency to optical fibers due to their circular output beam, on-wafer testing capability, integration, easy fabrication in large two-dimensional arrays, single-longitudinal mode operation, and high-speed modulation [9]. Enhancement of VCSEL characteristics can also be obtained by using optical injection [10]. For instance, injection locking [11], improvement of modulation bandwidth [12], and high-frequency microwave signal generation [13] can be obtained when the VCSEL is subjected to appropriate optical injection.

VCSELs also have additional degrees of freedom when compared to their edge-emitting counterparts like the direction of the emitted polarization. Due to their surface emission and cylindrical symmetry VCSELs lack strong polarization anisotropy and may undergo polarization switching (PS) when changing the temperature or bias current [9,23-26]. PS in VCSELs subject to optical injection has attracted considerable attention since the seminal work by Pan [14-22].

*aquirce@b-phot.com; phone +32 2 629 10 14

Semiconductor Lasers and Laser Dynamics VII, edited by Krassimir Panajotov, Marc Sciamanna, Angel Valle, Rainer Michalzik, Proc. of SPIE Vol. 9892, 98920Q · © 2016 SPIE
CCC code: 0277-786X/16/$18 · doi: 10.1117/12.2227786

Orthogonal optical injection is the usual technique for obtaining PS in optically-injected VCSELs [14-22]. In this technique linearly polarized light from a master laser is injected orthogonally to the linear polarization of the free-running VCSEL. Studies of PS in VCSELs subject to parallel optical injection, in which the directions of the linearly polarized light from the master laser and the slave VCSEL are parallel, are scarce: just a couple of experimental works have reported PS in VCSELs under these circumstances [21-22]. An analytical study of an optically injected two-polarization modes semiconductor laser has recently shown that pure and mixed-mode steady states can coexist [27]. Linear stability techniques have been used to analyze bistability between pure- and mixed-mode steady states [27].

In this work we make a theoretical and experimental analysis of the PS found in a single-transverse mode VCSEL subject to parallel optical injection. We report a state in which injection locking of the parallel polarization and excitation of the free-running orthogonal polarization of the VCSEL are simultaneously obtained. We will term this situation as IL+PS. This corresponds to the experimental observation in VCSELs of the mixed-mode steady states predicted in [27]. We obtain analytical expressions for the power of both linear polarizations in the IL+PS state. We show theoretically and experimentally that the power emitted in both linear polarizations depend linearly on the injected power. We also measure the stability region of the IL+PS state in the plane injected power versus frequency detuning.

The paper is organized as follows. In section 2, we describe the experimental setup. Section 3 and section 4 are devoted to the presentation of our experimental and theoretical results, respectively. Finally, in section 5, conclusions are presented.

2. EXPERIMENTAL SET-UP

We use an all-fiber experimental set-up shown in Fig. 1 to achieve parallel optical injection. Light from a tunable laser is injected into a 1550 nm quantum-well commercial VCSEL (Raycan Co.). The laser light is passed through a variable attenuator to adjust the injected power before the polarization is controlled with a polarization controller. We adjust polarization in a way that injection is achieved in the same polarization direction as the dominant VCSEL polarization. Optical injection is realized by a three port optical circulator. The power injected into the VCSEL is measured with a 50/50 optical coupler directing half of the injected power to a power meter. The bias current and temperature of the VCSEL are controlled by laser and temperature controllers, respectively. After port 3 of the circulator another polarization controller together with a polarization beam splitter are placed in order to measure power in both linear polarizations. Data acquisition is performed with either a power meter for each polarization or a high resolution (10 MHz) optical spectrum analyzer (BOSA).

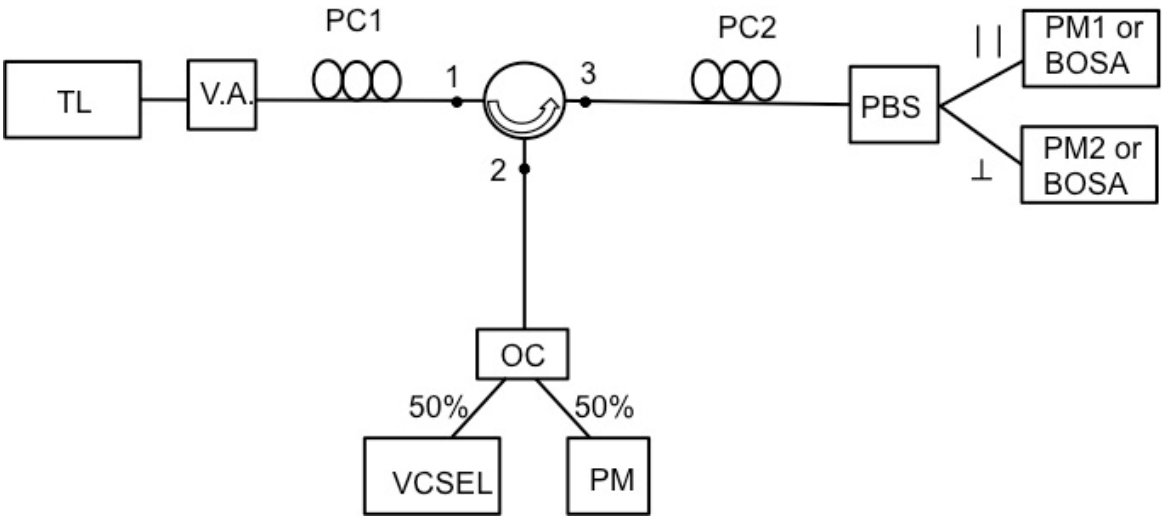

Figure 1. Experimental set-up for parallel optical injection. TL is a tunable laser; VA is a variable attenuator; PC1 and PC2 represent polarization controllers; PBS is a polarization beamsplitter; OC is a 50/50 optical coupler; PM, PM1 and PM2 are power meters; and BOSA is a high-resolution optical spectrum analyzer.

The free-running VCSEL emits in the fundamental transverse mode with a threshold current of I_{th} =1.66 mA at 25°C. The temperature and the bias current are held constant at 25°C and 3.05 mA, respectively. The solitary VCSEL emits in a linear polarization that we will call "x" or "parallel" polarization. The "orthogonal" or "y" polarization is 34 dB weaker than the parallel. The birefringence of the VCSEL is 33 GHz, corresponding to x and y wavelengths of λ_x=1540.91 nm and λ_y=1540.65 nm, respectively. Optical injection is characterized by its strength and by its frequency. The strength is given by the power measured in front of the VCSEL, P_i. The frequency is characterized by the frequency detuning, ν_i, defined as the difference between the injected frequency and the frequency of the solitary VCSEL.

3. EXPERIMENTAL RESULTS

We have measured the output power at both ports of the polarization beam splitter as a function of P_i. Results are shown in Fig. 2. The power measured at the parallel port of the PBS, P_{x+r}, includes the contributions of both the light emitted by the VCSEL and the reflection of the injected light at the VCSEL mirror. The power measured at the orthogonal port, P_y, is directly proportional to the power emitted by the VCSEL at the y-polarization. Fig. 2 shows that at low values of P_i the VCSEL emits in the x-polarization, as in the free-running situation. PS is observed at P_i=175μW because at this value P_y becomes much larger than P_{x+r}. Excitation of the y-polarization is maintained while 175μW < P_i < 1045 μW. Both P_y and P_{x+r} depend linearly on P_i. We have also measured the power in the parallel polarization, P_x. This is done by turning the VCSEL off and measuring the power in the parallel port of the PBS, P_r, for different values of P_i. P_r is the reflected power at the VCSEL mirror. If we assume that the phase difference between the fields corresponding to the light emitted by the VCSEL in the parallel polarization and the reflection at the VCSEL mirror of the injected light is very close to -90° or to 90°, P_x can be obtained by using $P_x = P_{x+r} - P_r$. This assumption will be checked at section 4. Fig. 2 also shows P_x and $P_{tot}=P_x+P_y$ as a function of P_i. P_x increases linearly in the interval 175μW < P_i < 1045 μW, in which PS has been observed. In this same interval we observe that P_{tot} is almost constant because it slightly increases, just a 3% from P_i=175 μW to P_i = 1045 μW.

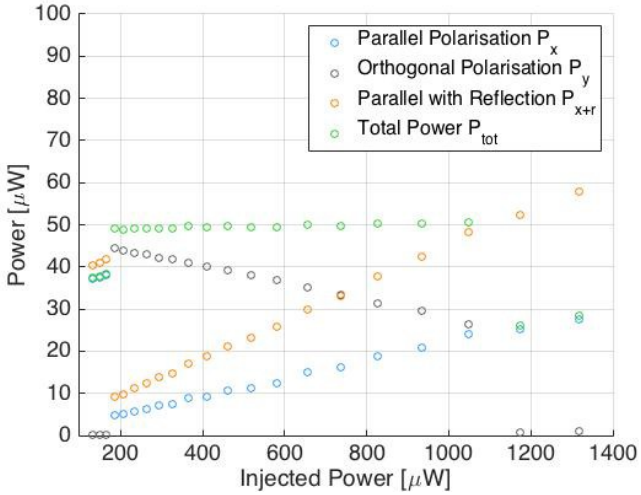

Figure 2. Experimental output powers as a function of the injected power, P_i. Results are shown for the power measured at the parallel port of the PBS (P_{x+r}), power of y-polarization (P_y), power of x-polarization (P_x) and total power (P_{tot}). The frequency detuning is ν_i = -8.6 GHz.

Figure 3 shows the experimental optical spectra of the total power as P_i is increased for a fixed value of ν_i = -8.4 GHz, very close to the detuning value considered in Fig. 2. The zero value of the frequency has been chosen to correspond to the x-polarization mode of the solitary VCSEL. Fig. 3(a) shows that the x-polarization mode experiences period-1 dynamics with a frequency equal to ν_i. This spectrum corresponds in Fig. 2 to a value of P_i in which PS has not been observed yet.

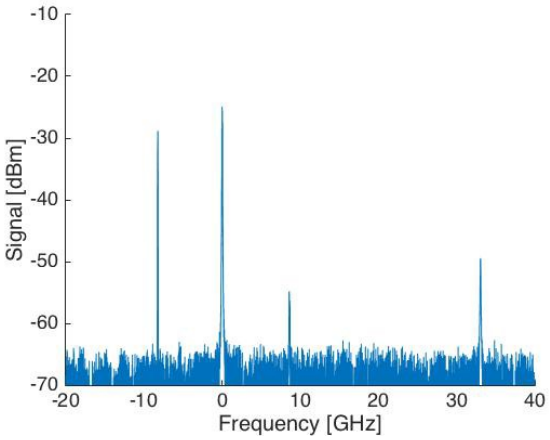

(a) P_i=133μW

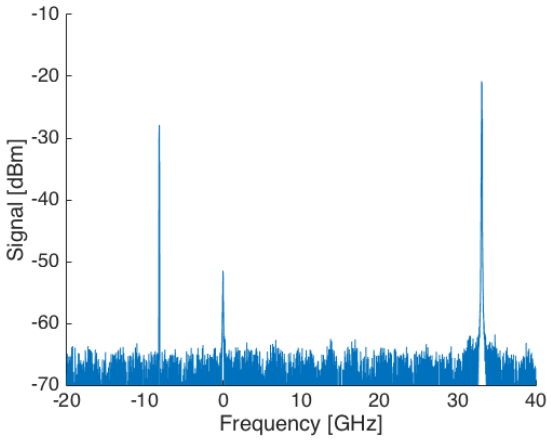

(b) P_i=209 μW

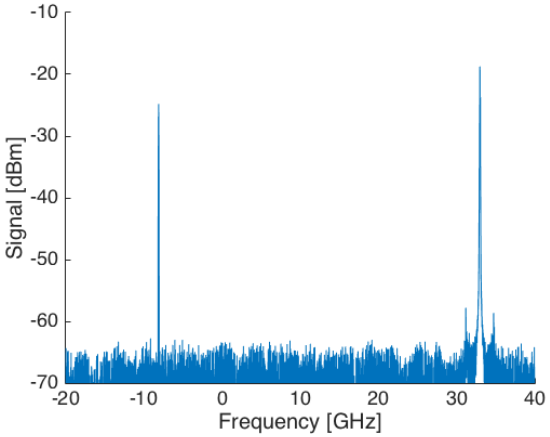

(c) P_i=416 μW

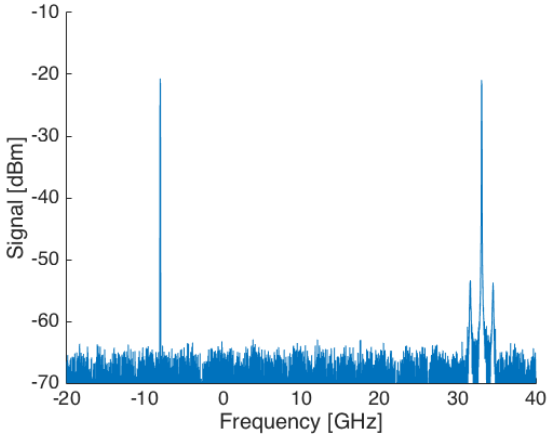

(d) P_i=833 μW

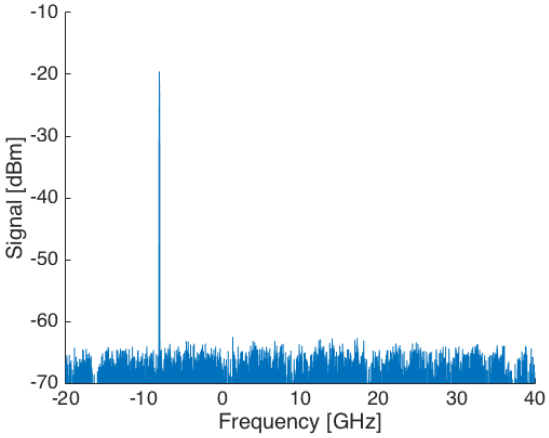

(e) P_i=1056μW

Figure 3. Experimental optical spectra corresponding to different values of P_i at a detuning of ν_i= -8.4 GHz.

Fig. 3(b) shows that when P_i increases PS is observed: the y (x) polarization mode is excited (suppressed) at its free-running frequency. Fig. 3(c) and Fig. 3(d) show injection locked emission in the x-polarization mode with a simultaneous excitation of the free-running y-polarization mode of the VCSEL. We denote this state as IL+PS.

Fig. 3(c) and Fig. 3(d) also show that the orthogonally polarized emission has two satellite peaks around the central peak. The frequency separation between the main and satellite peaks is slightly below the relaxation oscillation frequency, 2 GHz. Fig. 3(e) shows that injection locking in the parallel polarization without excitation of the orthogonal polarization mode is obtained at large enough values of P_i.

We now characterize in Fig. 4 the region of parameters space in which the IL+PS state is observed. For a fixed value of the frequency detuning we increase P_i from zero and record the range of injected powers in which the IL+PS is observed in the optical spectrum. Fig. 4 shows that there are two different regions, one at negative and another at positive values of ν_i, in which IL+PS is observed. Results analyzed in Fig. 2 and Fig. 3 correspond to the region of negative ν_i. The region that appears at positive ν_i values appears at lower values of P_i than those observed at negative ν_i values.

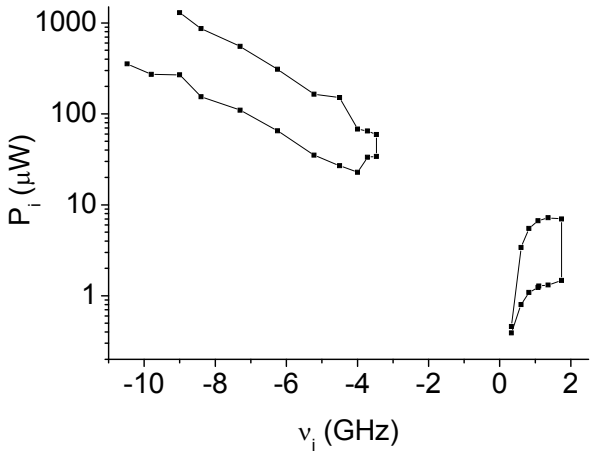

Figure 4. Experimental values of P_i for which IL+PS is observed as a function of ν_i.

4. THEORETICAL RESULTS

We now analyze the system from a theoretical point of view. We consider a rate equation model for the polarization modes of a single-transverse mode VCSEL based on the spin-flip model (SFM) [28]. In order to account for the parallel optical injection we introduce an injection term in the rate equation for the slowly varying component of the e-field in the x-direction. In this way the rate equations for SFM become:

$$\frac{dE_x}{dt} = -(\kappa + \gamma_a)E_x - i(\kappa\alpha + \gamma_p)E_x + \kappa(1 + i\alpha)(DE_x + inE_y) + \kappa E_{inj} e^{i2\pi\nu_{inj}t} \tag{1}$$

$$\frac{dE_y}{dt} = -(\kappa - \gamma_a)E_y - i(\kappa\alpha - \gamma_p)E_y + \kappa(1 + i\alpha)(DE_y - inE_x) \tag{2}$$

$$\frac{dD}{dt} = -\gamma\left[D(1 + |E_x|^2 + |E_y|^2) - \mu + in(E_y E_x^* - E_x E_y^*) \right] \tag{3}$$

$$\frac{dn}{dt} = -\gamma_s n - \gamma\left[n(|E_x|^2 + |E_y|^2) + iD(E_y E_x^* - E_x E_y^*) \right] \tag{4}$$

In these equations E_x, E_y are the two linearly polarized complex e-fields in the x and y directions, respectively, D is the total population inversion, and n is the difference between the population inversion for the spin-up and spin-down radiation channels. The parameters that appear in this model have been extracted for a similar free-running VCSEL [29-30]. Their meaning and values are the following: the field decay rate (κ=33ns^{-1}), the linear dichroism (γ_a=-0.1 ns^{-1}), the linewidth enhancement factor (α=2.8), the linear birefringence (γ_p=103.34 ns^{-1}), the decay rate of D (γ=2.08 ns^{-1}), the spin-flip relaxation rate (γ_s=2100 ns^{-1}) and the normalized bias current (μ=2.29) that corresponds to 3.05 mA. E_{inj} is the amplitude of the injected light. ν_{inj} is the detuning between the frequency of the injected light and the intermediate frequency between those of the x and y polarization, ν_x and ν_y, where $2\pi\nu_x=\alpha\gamma_a-\gamma_p$ and $2\pi\nu_y=\gamma_p-\alpha\gamma_a$, and therefore $\nu_i = \nu_{inj} - \nu_x$. Spontaneous emission noise terms have also been included in the calculations as in [31].

Fig. 5 shows the optical spectrum obtained for a frequency detuning similar to that of Fig. 3 when E_{inj}=0.99. Optical spectra corresponding to x and y polarization are plotted with black and red colour, respectively. These spectra are similar to those of Fig. 3(c) and Fig. 3(d), that illustrate IL+PS state. The peak that appears in the spectrum of the x-polarization at zero frequency disappears when neglecting the spontaneous emission noise. Satellite peaks appear for both optical spectra. Amplitude of these peaks is larger for the y-polarization, in agreement with our experimental results in which only satellite peaks are observed for this polarization. The frequency separation between the central and satellite peaks is 1.8 GHz, a slightly smaller value than the theoretical relaxation oscillation frequency, 2.1 GHz.

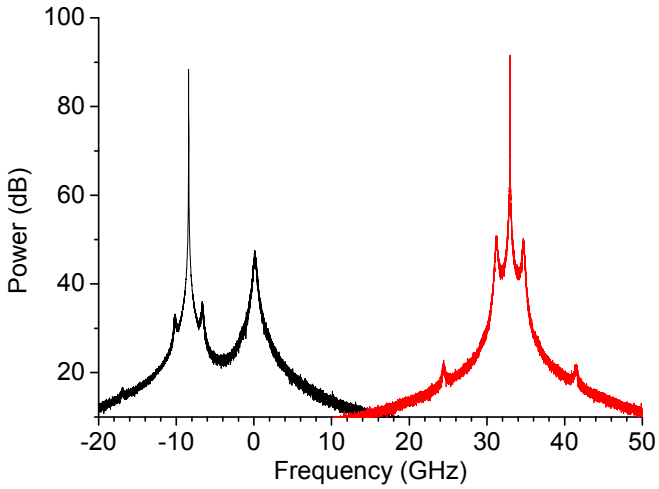

Figure 5. Theoretical optical spectrum illustrating the IL+PS state. Parameters are E_{inj}=0.99 and ν_i= -8.4 GHz. Black and red colors represent the x and y polarizations, respectively.

Simple analytical expressions can be derived from Eqs. (1)-(4) for the case of very large values of spin-flip relaxation rate. In our case this value is large (γ_s=2100 ns^{-1}) and therefore the n variable is very small. If we write $E_x(t)=A_x(t)\exp(i(2\pi\nu_{inj}t+\phi_x(t))$, $E_y(t)=A_y(t)\exp(i(2\pi\nu_y t+\phi_y(t))$, and make the approximation n=0 we obtain a set of rate equations for A_x , A_y , ϕ_x, ϕ_y and D. IL+PS solution is characterized by constant values of A_x and A_y , such that A_x>0, and A_y>0. Looking for this steady-state solution in the equation for A_y we get D=1- γ_a/κ, that is, the total population inversion is fixed to a value that does not depend on A_x nor ϕ_x. In this way, the fact that the depressed polarization mode is lasing provides a simple expression for the total population inversion D. Notice, that when a single-polarization mode is considered the carrier density is given by D=1+ γ_a/κ - $E_{inj}\cos(\phi_x)/A_x$, where A_x is found solving a third-order equation also involving ϕ_x. In this way considering two linear polarization modes in a model of a VCSEL subject to parallel optical injection leads to simpler expressions than those found for a VCSEL with only a single linear polarization.

Steady-state values can be found by making the temporal derivatives in the equations for A_x , ϕ_x, and D equal to zero and substituting D=1-γ_a/κ. We obtain the following simple expressions for the IL+PS state:

$$P_x = \left(\frac{\kappa}{2\gamma_a}\right)^2 \frac{P_{inj}}{1+\left(\frac{\pi\nu_i}{\gamma_a}+\alpha\right)^2} \tag{5}$$

$$P_x + P_y = \frac{\mu}{1-\gamma_a/\kappa} - 1 \tag{6}$$

$$\phi_x = -\arctan\left(\frac{\pi\nu_i}{\gamma_a}+\alpha\right) \tag{7}$$

where $P_{inj}=E_{inj}^2$, $P_x=A_x^2$, and $P_y=A_y^2$ are the power of the optical injection, x and y polarizations, respectively. Eq. (5) and Eq. (6) show that in the IL+PS state P_x and P_y depend linearly on P_{inj} , in agreement with the experimental results shown in Fig. 2. Substitution of the parameters of the model in Eq. (7) for the case of Fig. 2 gives ϕ_x=-89.79°. In this way we justify the approximation we did in Fig. 2 in order to obtain P_x. Eq. (6) also shows that $P_x + P_y$ is constant, independent of the injection parameters, P_{inj} and ν_i. This result is in agreement with the almost constant value of the experimental total power observed in Fig. 2.

5. CONCLUSIONS

In conclusion, we have investigated experimentally and theoretically the polarization switching found in a single-transverse mode VCSEL under parallel optical injection. We have obtained a novel state, IL+PS, characterized by simultaneous injection locking of the parallel polarization mode and excitation of the free-running orthogonal polarization mode of the VCSEL. This state has been experimentally characterized using the optical spectrum and the dependence of the power of both linear polarizations on the injected power. These powers depend linearly on the injected power in such a way that the total power is nearly constant. The stability region of IL+PS has been measured in the plane injected power versus frequency detuning. Theoretical results are obtained both from simulations of rate equations and from analytical expressions derived for the IL+PS. These expressions are very simple and describe well our experimental results.

ACKNOWLEDGMENTS

This work has been funded by the Ministerio de Economía y Competitividad, Spain under project TEC2015-65212-C3-1-P and cofinanced by FEDER funds. A. Quirce acknowledges FWO for her Post Doc fellowship and H. Thienpont and K. Panajotov are grateful to the Methusalem foundation for financial support.

REFERENCES

[1] J. Ohtsubo, [Semiconductor lasers: Stability, Instability, and Chaos], Springer Series in Optical Sciences (2007).
[2] M. Sciamanna, and K.A. Shore, "Physics and applications of laser diode chaos," Nature Photon. **9**, pp. 151-162 (2015).
[3] R. Lang, "Injection locking properties of a semiconductor laser," IEEE J. Quantum Electron. 18(6), 976-983 (1982).
[4] G. H. M. van Tartwijk, and D. Lenstra, "Semiconductor lasers with optical injection and feedback," Quantum Semiclass. Opt. **7**, 87-143 (1995).
[5] S. Wieczorek, B. Krauskopf, T. Simpson, and D. Lenstra, "The dynamical complexity of optically injected semiconductor lasers," Phys. Rep. 416, 1-128 (2005).

[6] X. Q. Qi, J. M. Liu, "Photonic microwave applications of the dynamics of semiconductor lasers," IEEE J. Sel. Topics Quantum Electron. 17(5), 1198-1211 (2011).
[7] S. C. Chan, "Analysis of an optically injected semiconductor laser for microwave generation," IEEE J. Quantum Electron. 46(3), 421-428 (2010).
[8] T. B. Simpson, J. M. Liu, M. Almulla, N. G. Usechak, V. Kovanis, "Linewidth sharpening via polarization-rotated feedback in optically injected semiconductor laser oscillators," IEEE J. Sel. Topics Quantum Electron. 19(4), 6415240 (2013).
[9] R. Michalzik, [VCSELs: fundamentals, technology, and applications of vertical-cavity surface-emitting lasers], Berlin, ed. Springer-Verlag (2012).
[10] F. Koyama, "Recent advances of VCSEL Photonics," J. Lightwave Technol. 24 (12), 4502-4513 (2006).
[11] H. Li, T. Lucas, J. G. McInerney, M. Wright, and R. A. Morgan, "Injection locking dynamics of vertical cavity semiconductor lasers under conventional and phase conjugate injection," IEEE J. Quantum Electronics. 32 (3), 227-235 (1996).
[12] C. H. Chang, L. Chrostowski, C. J. Chang-Hasnain, "Injection locking of VCSELs," IEEE J. Select. Topics Quantum Electron. 9 (5), 1386-1393 (2003).
[13] A. Quirce, A. Valle, "High-frequency microwave signal generation using multi-transverse mode VCSELs subject to two-frequency optical injection," Opt. Exp. 20 (12), 13390-13401 (2012).
[14] Z. G. Pan, S. Jiang, M. Dagenais, R. A. Morgan, K. Kojima, M. T. Asom, and R. E. Leibenguth, "Optical injection induced polarization bistability in vertical-cavity surface-emitting lasers," Appl. Phys. Lett. 63 (22), 2999-3001 (1993).
[15] J. Buesa, I. Gatare, K. Panajotov, H. Thienpont, and M. Sciamanna, "Mapping of the dynamics induced by orthogonal optical injection in vertical-cavity surface-emitting lasers," IEEE J. Quantum Electron. 42(2), 198-207 (2006).
[16] M. Sciamanna, and K. Panajotov, "Route to polarization switching induced by optical-injection in vertical-cavity surface-emitting lasers," Phys. Rev. A. 73(2), 023811 (2006).
[17] K. Panajotov, I. Gatare, A. Valle, H. Thienpont and M. Sciamanna, "Polarization- and Transverse-Mode Dynamics in Optically Injected and Gain-Switched Vertical-Cavity Surface-Emitting Lasers," IEEE J. Quantum Electron. 45 (11), 1473-1481 (2009).
[18] Y. Hong, K.A. Shore, A. Larsson, M. Ghisoni, and J. Halonen, "Pure frequency-polarisation bistability in vertical-cavity surface-emitting lasers subject to optical injection," Electron. Lett. 36 (24), 2019-2020 (2000).
[19] I. Gatare, K. Panajotov, M. Sciamanna, "Frequency-induced polarization bistability in vertical-cavity surface-emitting lasers with orthogonal optical injection," Phys Rev. A. 75, 023804 (2007).
[20] A. Hurtado, A. Quirce, A. Valle, L. Pesquera, and M. J. Adams, "Nonlinear dynamics induced by parallel and orthogonal optical injection in 1550 nm vertical-cavity surface-emitting lasers (VCSELs)," Opt. Exp. 18 (9), 9423-9428 (2010).
[21] A. Qader, Y. Hong, and K.A. Shore, "Role of suppressed mode in the polarization switching characteristics of optically injected VCSELs," IEEE J. Quantum Electron., 49, (2), 205-210 (2013).
[22] Y. Hong, K. A. Shore, A. Larsson, M. Ghisoni, and J. Halonen, "Polarisation switching in a vertical-cavity surface emitting semiconductor laser by frequency detuning," IEE Proc.-Optoelectron. 148, (1), 31-34 (2001).
[23] K. D. Choquette, R.P. Schneider, K. L. Lear, and R. E. Leibenguth, "Gain-dependent polarization properties of vertical-cavity lasers," IEEE J. Sel. Top. Quantum Electron. 1 (2), 661-666 (1995).
[24] M. San Miguel, Q. Feng and J. V. Moloney, "Light-Polarization Dynamics in Surface-Emitting Semiconductor-Lasers,"Physical Review A, 52 (2), 1728-1739 (1995).
[25] B. Ryvkin, K. Panajotov, A. Georgievski, J. Danckaert, M. Peeters, G. Verschaffelt, H. Thienpont, and I. Veretennicoff, "Effect of photon-energy dependent loss and gain mechanisms on polarization switching in vertical cavity surface-emitting lasers," J. Opt. Soc. Amer. B,16 (11), 2106-2113 (1999).
[26] A. Valle, L. Pesquera, and K. A. Shore, "Polarization behavior of birefringent multitransverse mode vertical-cavity surface-emitting lasers," IEEE Photon. Technol. Lett., 9 (5), 557-559 (1997).
[27] G. Friart, A. Gavrielides, and T. Erneux, "Analytical stability boundaries of an injected two-polarization semiconductor laser," Phys. Rev. E, 91, 042918 (2015).
[28] J. Martin-Regalado, F. Prati, M. San Miguel, and N. B. Abraham, "Polarization properties of vertical-cavity surface-emitting lasers," IEEE J. Quantum Electron. 33(5), 765-783 (1997).
[29] P. Perez, A. Valle, L. Pesquera, "Measurement of the intrinsic parameters of single-mode VCSELs," J. Lightw. Technol. 32 (8), 1601-1607 (2014).

[30] P. Perez, A. Valle, L. Pesquera, "Polarization-resolved characterization of long-wavelength vertical-cavity surface-emitting laser parameters," J. Opt. Soc. Am. B, 31 (11), 2574-2580 (2014).
[31] P. Perez, A. Quirce, A. Valle, A. Consoli, I. Noriega, L. Pesquera, I. Esquivias, "Photonic generation of microwave signals using a single-mode VCSEL subject to dual-beam ortogonal optical injection," IEEE Phot. Journal, 7 (1), 5500614 (2015).